## ORIGINAL ARTICLE

# Integrative taxonomy unveils a new species of *Dugesia* (Platyhelminthes, Tricladida, Dugesiidae) from the southern portion of the Taihang Mountains in northern China, with the description of its complete mitogenome and an exploratory analysis of mitochondrial gene order as a taxonomic character

Lei WANG,[1,3] Yixuan WANG,[1] Zimei DONG,[1] Guangwen CHEN,[1] Ronald SLUYS[2] and Dezeng LIU[1]

[1]College of Life Science, Henan Normal University, Xinxiang, China, [2]Naturalis Biodiversity Center, Leiden, The Netherlands and [3]Medical College, Xinxiang University, Xinxiang, China

## Abstract

A new species of *Dugesia* (Platyhelminthes, Tricladida, Dugesiidae) from northern China is described on the basis of an integrative approach, involving morphology, karyology, histology, molecular distance, molecular phylogeny, and mitochondrial gene order. Here, we present the complete mitogenome of the new species *Dugesia constrictiva* Chen & Dong, **sp. nov**. This new species is mainly characterized by the presence of the following features: asymmetrical openings of the oviducts; large, cuboidal copulatory bursa; vasa deferentia opening through the ventro-lateral wall of the seminal vesicle; laterally compressed seminal vesicle; ventrally displaced ejaculatory duct, opening at the blunt tip of the penis papilla; long duct intercalated between seminal vesicle and diaphragm; chromosome complement diploid, with 16 metacentric chromosomes; mitochondrial gene order as follows: *cox1-E-nad6-nad5-S2-D-R-cox3-I-Q-K-atp6-V-nad1-W-cox2-P-nad3-A-nad2-M-H-F-rrnS-L1-Y-G-S1-rrnL-L2-T-atp8-C-N-cob-nad4l-nad4*. In triclads, mitochondrial gene order is considerably conserved between freshwater planarians and land flatworms, whereas it is variable between marine planarians and both freshwater and land flatworms. The secondary structures of tRNAs are all equipped with 4 arms, excepting *tRNA S1* and *tRNA S2*, which lack the D arm and have excessively enlarged loops. Numerous transpositions of tRNA are present between *D. constrictiva* and its congeners. Mitochondrial gene arrangements may form a new, additional tool for taxonomic studies. The phylogenetic tree based on analysis of the mitochondrial genome basically corroborates current classification of the higher taxa of planarian flatworms.

**Key words:** *Dugesia*, mitochondrial genome, new species, taxonomy

*Correspondence*: Guangwen Chen and Zimei Dong, College of Life Science, Henan Normal University, Xinxiang, Henan 453007, China.
Email: chengw0183@sina.com; dzmhjx@163.com

## INTRODUCTION

The Taihang Mountains in China are located at the eastern margin of the Loess Plateau, the latter bordering on the immense North China Plain or Tibetan Plateau, which experienced during its geological history multiple periods of structural orogenic processes, such as the Yanshanian, Himalayan, and Lüliangshian processes (Zhong*et al*. 2010; Lin *et al*. 2020). Furthermore, the Taihang Mountains form one of the regions with the most abundant and rich animal diversity in China (Wang *et al*. 2009; Raorao *et al*. 2019), from which previously 2 species of the planarian genus *Polycelis* Ehrenberg, 1831 have been reported (Chen *et al*. 2008; Dong *et al*. 2017). In the present paper, we describe a third, new species of freshwater planarian from the Taihang Mountains, namely, a representative of the genus *Dugesia* Girard, 1850, on the basis of an integrative approach involving morphology, karyology, histology, molecular distance, and molecular phylogeny. Members of this genus are widely distributed in the Old World and Australia (Sluys & Riutort 2018, fig. 13B), with only 7 species presently being known from China, namely, *Dugesia japonica* Ichikawa & Kawakatsu, 1964, *D. sinensis* Chen & Wang, 2015, *D. umbonata* Song & Wang, 2020, *D. semiglobosa* Chen & Dong, 2021, *D. majuscula* Chen & Dong, 2021, *D. circumcisa* Chen & Dong, 2021, and *D. verrucula* Chen & Dong, 2021 (Kawakatsu *et al*. 1976; Chen *et al*. 2015; Song *et al*. 2020; Wang *et al*. 2021a,b). Only 5 of these Chinese species were recorded from mainland China, since *D. semiglobosa* and *D. majuscula* are known only from Hainan Island.

For the present study, we apply a new sequencing method, at least for planarians, that enabled us to assemble the complete mitochondrial genome of the new species of *Dugesia* described herein. This is compared with the few other complete as well as incomplete sequences for triclads that have already been published and are currently available from GenBank. In this way, we explore a new dataset that potentially comprises abundant molecular information for resolving phylogenetic relationships among flatworms (Solà *et al*. 2015; Kenny *et al*. 2018). Furthermore, widely conserved regions and unexpectedly divergent blocks in the arrangement of the mitochondrial gene order may be instrumental in deducing variation among planarian species (Solà *et al*. 2015; Egger *et al*. 2017; Monnens *et al*. 2020) and, thus, may potentially form a new set of taxonomic characters.

## MATERIALS AND METHODS

### Specimen collection and culturing

Specimens were directly collected with a brush from under stones in a spring in northern China (35°43′5″N, 114°6′32″E; Fig. 1) on October 16, 2018. The worms were transferred to plastic bottles filled with spring water, which were placed in a cooler filled with an ice bag during transportation to the laboratory. The planarians were cultured in autoclaved tap water at 16°C and fed with fresh beef liver once per week. The worms were starved for at least 1 week before being used for karyotype studies, histological studies, and extraction of nuclear and mitochondrial DNA. Images of their external morphology were obtained by using a digital camera attached to a stereo-microscope.

### Histology and karyology

For preparation of histological sections, the worms were fixed in Bouin's fluid for 24 h, and, subsequently, rinsed and stored in 70% ethanol. Hereafter, specimens were dehydrated in an ascending series of ethanol solutions, after which they were cleared in clove oil and embedded in synthetic paraffin. Serial sections were made at intervals of 6 $\mu$m and were stained with hematoxylin-eosin. Photomicrographs were taken with a Leica digital camera attached to a compound microscope. Histological preparations of specimens have been deposited in the Zoological Museum of the College of Life Science of Henan Normal University (ZMHNU), Xinxiang, China and Naturalis Biodiversity Center, Leiden, The Netherlands (RMNH). Living specimens were cultured in the laboratory.

Karyological preparations were obtained by the air-drying method. The worms were first cut transversally into 3 pieces, which were cultured in distilled water for 3 days. Regenerative blastemas were treated with a 0.02% colchicine solution at 13°C for 2.5–3.5 h and then placed in 0.1% KCl hypotonic solution at 16°C for approximately 2.0–3.5 h. Hereafter, the blastemas were washed with deionized water and then fixed on a slide for about 30 s in each of the following solutions: fixative fluid I (glacial acetic acid: absolute alcohol: deionized water in the ratio of 3:3:4), fixative fluid II (glacial acetic acid: absolute alcohol in the ratio of 1:1), and fixative fluid III (glacial acetic acid). Subsequently, the dispersed cells were dried at room temperature for 24 h, and stained with a 0.5% Giemsa solution for 12–15 min.
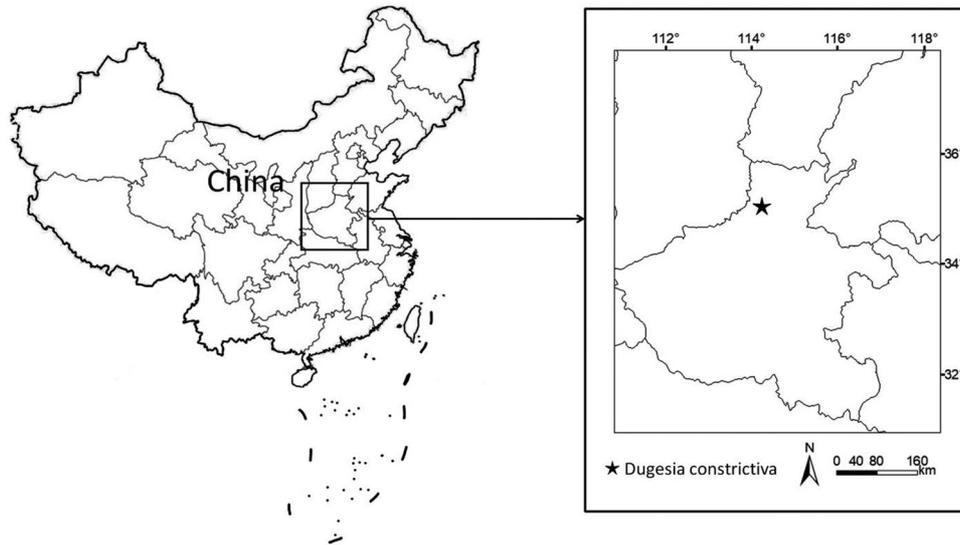
**Figure 1** Collection site of *Dugesia constrictiva* in the Taihang Mountains.

The mitotic metaphase chromosomes were observed and photographed under a compound microscope equipped with a digital camera. Well-spread sets of metaphase plates from different and random individuals were used for karyotype analysis; karyotype parameter measurements were carried out as described previously Chen *et al.* (2008). Chromosomal nomenclature follows Levan *et al.* (1964).

## DNA extraction, amplification, sequencing, and phylogenetic analysis

Total genomic DNA was extracted from specimens by using the QIAamp® DNA Mini Tissue Kit (Qiagen, Germany), according to the manufacturer's protocols. Fragments of the Cytochrome C oxidase subunit I (COI) and internal transcribed spacer-1 (ITS-1) were amplified using specific primers (sequences and annealing temperatures are listed in Table S1, Supporting Information). Premix Ex Taq$^{TM}$ Hot Start Version (TaKaRa, Otsu, Japan) was used for the polymerase chain reaction (PCR). Amplifications were conducted in a final volume of 30 $\mu$L under the following conditions: 5 min at 94°C, 35 cycles of 40 s at 94°C, an annealing step for 30 s, and 1 min at 72°C and 5 min at 72°C as a final extension. Purification of PCR products and sequencing were done by GENEWIZ (Tianjin, China). Sequencing reactions were performed with the same primers used to amplify the fragments. All specimens were sequenced for both forward and reverse DNA strands, while chromatograms were visually checked. Six specimens were used to extract nuclear and mitochondrial DNA, while COI and ITS-1 were amplified.

In order to determine whether the presumed new species was molecularly different from its congeners, we performed a phylogenetic analysis and calculated genetic distances. The ingroup included the new species and 30 other *Dugesia* species from major portions of the geographic range of the genus, while, *Schmidtea mediterranea* (Benazzi *et al.*, 1975) was used as an outgroup taxon (for GenBank accession numbers, see Table 1).

Nuclear ribosomal markers were aligned online with MAFFT (Online Version 7.247) using the G-INS-i algorithm (Katoh & Standley 2013), and were checked by using BioEdit 7.2.6.1. The Translator X pipeline was used to align the protein-coding COI sequences (http://translatorx.co.uk; Abascal *et al.* 2010). Nucleotide sequences were translated to amino acid sequences with the help of NCBI's genetic codes Translation Table 9, followed by MAFFT (Online Version 7.247) using FFT-NS-2 progressive alignment method, and checked by using BioEdit 7.2.6.1, and then back-translated to nucleotide sequences. Since automated removal of gap columns and variable regions has been reported to negatively affect the accuracy of the inferred phylogeny (Dessimoz & Gil 2010; Tan *et al.* 2015), the Gblocks (Talavera & Castresana 2007) option was disabled. The concatenated data in our dataset for the phylogenetic analysis were in the order ITS-1 + COI and consisted of a total of 1547 bp, including 5.19% missing data. In the concatenated dataset, missing data had been marked as "?".

**Table 1** GenBank accession numbers of COI and ITS-1 sequences used for molecular analysis

| Species | GenBank | |
| --- | --- | --- |
| | COI | ITS-1 |
| *D. aethiopica* | KY498845 | KY498785 |
| *D. afromontana* | KY498846 | KY498786 |
| *D. arcadia* | KC006971 | KC007044 |
| *D. ariadnae* | KC006972 | KC007048 |
| *D. batuensis* | KF907818 | KF907815 |
| *D. benazzii* | FJ646977 + FJ646933 | FJ646890 |
| *D. bengalensis* | | FJ646897 |
| *D. bifida* | KY498851 | KY498791 |
| *D. circumcisa* | MZ147041 | MZ146782 |
| *D. cretica* | KC006976 | KC007050 |
| *D. constrictiva* | MZ871766 | MZ869023 |
| *D. deharvengi* | KF907820 | KF907817 |
| *D. elegans* | KC006984 | KC007063 |
| *D. etrusca* | FJ646984 + FJ646939 | FJ646898 |
| *D. gibberosa* | KY498857 | KY498803 |
| *D. gonocephala* | FJ646986 + FJ646941 | FJ646901 |
| *D. hepta* | FJ646988 + FJ646943 | FJ646902 |
| *D. japonica* | FJ646990 | FJ646904 |
| *D. liguriensis* | FJ646992 | FJ646907 |
| *D. majuscula* | MW533425 | MW533591 |
| *D. naiadis* | KF308756 | |
| *D. notogaea* | FJ646993 + FJ646945 | FJ646908 |
| *D. ryukyuensis* | AF178311 | FJ646910 |
| *D. sagitta* | KC007006 | KC007077 |
| *D. semiglobosa* | MW525210 | MW526992 |
| *D. sicula* | FJ646994 + FJ646947 | DSU84356 |
| *D. sigmoides* | KY498849 | KY498789 |
| *D. sinensis* | KP401592 | |
| *D. subtentaculata* | FJ646995 + FJ646949 | DSU84369 |
| *D. umbonata* | MT176641 | MT177211 |
| *D. verrucula* | MZ147040 | MZ146760 |
| *S. mediterranea* | JF837062 | AF047854 |

Mr Bayes v 3.2 (Ronquist *et al.* 2012) and RaxML 8.2.10 (Stamatakis 2014) were used to infer phylogenies with the Bayesian inference (BI) and maximum-likelihood (ML) method, respectively. BI was run for 3 million generations and 25% burn-in was used under the GTR + I + G model. For the ML analysis, we performed 10 000 replicates with the GTR + I + G model. BI and ML trees were visualized and edited using Figtree v1.4.3.

The genetic distances of COI and ITS-1 were calculated using MEGA 6.06 (Tamura *et al.* 2013) with the Kimura 2-parameter substitution model (Lázaro *et al.* 2009; Solà *et al.* 2013).

## Preparation of a clonal strain for mitochondrial genome extraction

After having reached sexual maturity, a single worm was cut into 2 fragments anterior to the pharynx. The posterior portion of the body including pharynx and copulatory apparatus was used for histological study, while the anterior portion was utilized for a kind of clonal propagation, in that it was divided into 5 pieces, which regenerated to complete specimens that were used for mitochondrial DNA extraction.

## Mitochondrial DNA extraction and sequencing

Mitochondrial DNA extraction, sequencing, genome assembly, and annotation were conducted by Shanghai BIOZERON Co., Ltd (Shanghai, China). Briefly, mitochondrial genomic DNA was isolated from each of the 5 regenerated clonal specimens of *Dugesia constrictiva* by animal mitochondrial DNA column extraction kit (Sequencing Grade, BioRab, China), according to the manufacturer's protocols. The mitochondrial genome was sequenced by using a combination of the PacBio RS and Illumina sequencing platforms. In Illumina pair-end sequencing, at least 3 $\mu$g genomic DNA was used for the construction of the library of sequences. The certified Illumina pair-end library was sequenced on Illumina NovaSeq 6000 (2 × 150 bp paired-end reads). For PacBio RS sequencing, 20k insert whole genome shotgun libraries were generated and sequenced on a Pacific Biosciences RS instrument using standard methods.

## Mitochondrial genome assembly and annotation

Mitochondrial genome was sequenced using a combination of PacBio RS and Illumina sequencing platforms. The Illumina data was used to evaluate the complexity of the genome and corrected the PacBio long-reads. ABySS (http://www.bcgsc.ca/platform/bioinfo/software/abyss, v2.0.2) was used to perform genome assembly, with multiple-Kmer parameters in order to obtain optimal results of the assembly. RlasR was used to map the preliminary assembly results to the PacBio long reads. Then, SPAdes-3.10.1 was used to assemble Pacbio and Illumina data in order to construct contigs (Scaffolds). GapCloser software (http://soap.genomics.org.cn/soapdenovo.html) was applied to fill up the remaining local inner gaps and to correct for single base polymorphism, thus obtaining the final assembly results.

The mitochondrial genes were annotated using homologous alignments and *de novo* prediction. The secondary structures of mitochondrial transfer RNA (tRNA) genes were predicted by tRNAscan-SE (http://lowelab.ucsc.edu/tRNAscan-SE/) and MITOS (http://mitos2.bioinf.uni-leipzig.de/index.py), while the ribosomal RNA (rRNA) genes and protein coding genes were used to make homologous alignments with the mitochondrial genomes of Polycladida and Tricladida as reference genome (Table S2, Supporting Information). The circular diagram of the mitochondrial genome was developed with Organellar Genome DRAW (http://ogdraw.mpimp-golm.mpg.de/cgi-bin/ogdraw.pl).

## Mitochondrial phylogenetic analysis

For phylogenetic analysis of flatworm taxa, a dataset was created including mitochondrial protein-coding genes and ribosomal genes (excepting *atp8*) from several major taxa of the phylum Platyhelminthes, as well as from the phylum Gnathostomulida (for GenBank accession numbers, see Table 2). *Gnathostomula armata* was used as outgroup because there is a close phylogenetic relationship between Gnathostomulida and Platyhelminthes (Littlewood *et al*. 1998; Kenny *et al*. 2018). The nucleotide sequences of each individual gene were aligned by using the program MAFFT (Online Version 7.247), using the FFT-NS-i model. Alignments were individually analyzed with Gblocks under 3 "relaxed" parameters (smaller final blocks, gap positions within the final blocks, and less strict flanking positions allowed), excluding from further analysis ambiguously aligned and excessively variable regions (Castresana 2000). FASconCAT was then used to combine the alignments (Kück & Meusemann 2010). Maximum likelihood (ML) analysis was conducted, using RAxML version 8.2.10 with 1000 bootstrap replicates under the GTR + I + G model. For Bayesian inference (BI) analysis, Mr Bayes v 3.2 was run for 3 million generations under the GTR + I + G model and with 25% burn-in. BI and ML trees were visualized and edited using Figtree v1.4.3.

## Ethics statement

This study was not involve endangered or protected species, and the collection of specimens was approved by the Forestry Department of Wild Animal Protection, Henan Province, China. All handling procedures were strictly compliant with the current Animal Protection Law of China, and the studies had been approved by the research ethics committee at the Henan Normal University.

**Table 2** Species, classification, and corresponding GenBank accession numbers of mitochondrial genomes used for mitochondrial analysis

| Species | Classification | GenBank |
|---|---|---|
| *Gnathostomula armata* | Gnathostomulida; Bursovaginoidea; Gnathostomulidae | KP965860 |
| *Stenostomum sthenum* | Platyhelminthes; Catenulida; Stenostomidae; Stenostomum | MF078638 |
| *Macrostomum lignano* | Platyhelminthes; Rhabditophora; Macrostomorpha; Macrostomida; Macrostomidae; Macrostomum | NC_035255 |
| *Graffilla buccinicola* | Platyhelminthes; Rhabditophora; Rhabdocoela; Dalyellioida; Graffillidae; | NC_050390 |
| *Syndesmis echinorum* | Platyhelminthes; Rhabditophora; Rhabdocoela; Dalyellioida; Umagillidae; | NC_050392 |
| *Syndesmis karukaikina* | Platyhelminthes; Rhabditophora; Rhabdocoela; Dalyellioida; Umagillidae; | NC_050391 |
| *Cryptocelis alba* | Platyhelminthes; Rhabditophora; Polycladida; Acotylea; Leptoplanoidea; Cryptocelidae | MF993331 |
| *Hoploplana elisabelloi* | Platyhelminthes; Rhabditophora; Polycladida; Acotylea; Leptoplanoidea; Leptoplanidae | KT363735 |
| *Notocomplana palta* | Platyhelminthes; Rhabditophora; Polycladida; Acotylea; Leptoplanoidea; Notoplanidae | MF993337 |
| *Stylochoplana maculata* | Platyhelminthes; Rhabditophora; Polycladida; Acotylea; Leptoplanoidea; Stylochoplanidae | KP965863 |
| *Crassiplana albatrosi* | Platyhelminthes; Rhabditophora; Polycladida; Acotylea; Stylochoidea; Callioplanidae | MF993330 |
| *Imogine stellae* | Platyhelminthes; Rhabditophora; Polycladida; Acotylea; Stylochoidea; Stylochidae | MF993336 |
| *Planocera reticulata* | Platyhelminthes; Rhabditophora; Polycladida; Acotylea; Stylochoidea; Planoceridae; | NC_036051 |
| *Eurylepta cornuta* | Platyhelminthes; Rhabditophora; Polycladida; Cotylea; Euryleptoidea; Euryleptidae | MF993334 |
| *Enchiridium* sp. | Platyhelminthes; Rhabditophora; Polycladida; Cotylea; Euryleptoidea; Prosthiostomidae | KT363734 |
| *Prosthiostomum siphunculus* | Platyhelminthes; Rhabditophora; Polycladida; Cotylea; Euryleptoidea; Prosthiostomidae | KT363736 |
| *Obrimoposthia wandeli* | Platyhelminthes; Rhabditophora; Seriata; Tricladida; Maricola; Bdellouroidea; Uteriporidae; Ectoplaninae | NC_050050 |
| *Crenobia alpina* | Platyhelminthes; Rhabditophora; Seriata; Tricladida; Continenticola; Planarioidea; Planariidae; | KP208776 |
| *Phagocata gracilis* | Platyhelminthes; Rhabditophora; Seriata; Tricladida; Continenticola; Planarioidea; Planariidae | KP090060 |
| *Bipalium kewense* | Platyhelminthes; Rhabditophora; Seriata; Tricladida; Continenticola; Geoplanoidea; Geoplanidae; Bipaliinae; | NC_045216 |
| *Obama* sp. | Platyhelminthes; Rhabditophora; Seriata; Tricladida; Continenticola; Geoplanoidea; Geoplanidae; Geoplaninae | KP208777 |
| *Dugesia constrictiva* | Platyhelminthes; Rhabditophora; Seriata; Tricladida; Continenticola; Geoplanoidea; Dugesiidae | OK078614 |
| *Dugesia japonica* | Platyhelminthes; Rhabditophora; Seriata; Tricladida; Continenticola; Geoplanoidea; Dugesiidae | AB618487 |
| *Dugesia ryukyuensis* | Platyhelminthes; Rhabditophora; Seriata; Tricladida; Continenticola; Geoplanoidea; Dugesiidae | AB618488 |
| *Girardia* sp. | Platyhelminthes; Rhabditophora; Seriata; Tricladida; Continenticola; Geoplanoidea; Dugesiidae | KP090061 |
| *Schmidtea mediterranea* | Platyhelminthes; Rhabditophora; Seriata; Tricladida; Continenticola; Geoplanoidea; Dugesiidae | KM821047 |
| *Benedenia hoshinai* | Platyhelminthes; Monogenea; Monopisthocotylea; Capsalidae | NC_014591 |
| *Gyrodactylus derjavinoides* | Platyhelminthes; Monogenea; Monopisthocotylea Gyrodactylidae | NC_010976 |
| *Microcotyle sebastis* | Platyhelminthes; Monogenea; Polyopisthocotylea; Microcotylidae | NC_009055 |

*(Continued)*

**Table 2** (Continued)

| Species | Classification | GenBank |
| --- | --- | --- |
| *Diphyllobothrium latum* | Platyhelminthes; Cestoda; Eucestoda; Diphyllobothriidea; Diphyllobothriidae | AB269325 |
| *Taenia saginata* | Platyhelminthes; Cestoda; Eucestoda; Cyclophyllidea; Taeniidae | NC_009938 |
| *Clonorchis sinensis* | Platyhelminthes; Trematoda; Digenea; Opisthorchiida; Opisthorchiata; Opisthorchiidae | NC_012147 |
| *Schistosoma mansoni* | Platyhelminthes; Trematoda; Digenea; Strigeidida; Schistosomatoidea; Schistosomatidae | NC_002545 |
| *Schistosoma japonicum* | Platyhelminthes; Trematoda; Digenea; Strigeidida; Schistosomatoidea; Schistosomatidae | HM120848 |

## RESULTS

### Molecular phylogeny of COI and ITS-1

From 6 specimens, the final fragments of the nuclear ribosomal gene ITS-1 and the mitochondrial gene COI are 702 and 845 base pairs (bp), respectively. There is no variation in COI and ITS-1 among the 6 specimens' sequences.

The phylogenetic trees and their supporting values from the analysis of the concatenated dataset for both ML and BI show similar topologies and supported nodes, differing only in nodes weakly supported in at least one of the methodologies (Fig. 2; Fig. S1, Supporting Information). In the Bayesian tree, most nodes are supported by a posterior probability (pp) ≥ 0.95 and a bootstrap (bs) value ≥90 (Fig. 2). The new species occupies a separate branch, while it shares a sister-group relationship with *D. verrucula*. The clade *D. constrictiva* & *D. verrucula* & *D. majuscula* is sister to *D. japonica*.

### Genetic distances

The separate species status of *D. constrictiva* is supported also by our analysis of the genetic distances between the species, albeit that the distances of both COI and ITS-1 vary greatly among species (Table 3). The highest COI and ITS-1 distance values between *D. constrictiva* and its Oriental-Australasian congeners are 26.77% and 13.64%, respectively (with *D. deharvengi* and *D. notogaea*). Furthermore, the lowest COI and ITS-1 distance values of *D. constrictiva* are with *D. verrucula*, being 16.58% and 2.61%, respectively. The COI distance value between *D. constrictiva* and *D. japonica* is 20.07%, while the ITS-1 distance value is 6.82% (Table 4).

### Mitochondrial genome

The combination of PacBio RS and Illumina sequencing provide sufficient information for assembling the mitochondrial genome of *D. constrictiva*, which is 17 634 bp in length and includes 13 protein-coding genes, 22 tRNA genes, and 2 ribosomal genes. The ribosomal genes are located close to the long non-coding region (Fig. 3). GC content is 28.69%, and its GC Skew is showed in Fig. 3. The noncanonical *atp8* is located between *rrnL* and *cob* (Fig. 4) and provides with one transmembrane domain, while its first 4 amino acids are "MKYM" (Fig. S2, Supporting Information). The secondary structures of the mitochondrial tRNAs of *D. constrictiva* show that

**Table 3** Genetic distances for COI between the new species and its congeners

| | *S. mediterranea* | *D. batuensis* | *D. deharvengi* | *D. notogaea* | *D. japonica* | *D. ryukyuensis* | *D. sinensis* | *D. umbonata* | *D. circumcisa* | *D. verrucula* | *D. semiglobosa* | *D. majuscula* | *D. constrictiva* |
|---|---|---|---|---|---|---|---|---|---|---|---|---|---|
| *S. mediterranea* | | | | | | | | | | | | | |
| *D. batuensis* | 46.25% | | | | | | | | | | | | |
| *D. deharvengi* | 40.57% | 16.23% | | | | | | | | | | | |
| *D. notogaea* | 37.34% | 16.76% | 16.31% | | | | | | | | | | |
| *D. japonica* | 41.83% | | | 22.13% | | | | | | | | | |
| *D. ryukyuensis* | 38.31% | 13.77% | 15.92% | 14.40% | | | | | | | | | |
| *D. sinensis* | 37.98% | 26.65% | 23.18% | 18.27% | 22.75% | 25.29% | | | | | | | |
| *D. umbonata* | 35.23% | 22.21% | 19.85% | 15.61% | 17.11% | 20.61% | 14.59% | | | | | | |
| *D. circumcisa* | 35.61% | 24.65% | 23.67% | 17.56% | 19.94% | 20.99% | 15.98% | 11.20% | | | | | |
| *D. verrucula* | 39.56% | 21.73% | 24.15% | 21.83% | 17.66% | 22.60% | 20.70% | 15.47% | 17.15% | | | | |
| *D. semiglobosa* | 35.94% | 14.19% | 16.22% | 16.89% | 20.89% | 14.54% | 14.00% | 10.71% | 12.31% | 19.08% | | | |
| *D. majuscula* | 39.86% | 16.16% | 14.12% | 17.42% | 22.16% | 18.63% | 19.08% | 16.20% | 17.55% | 15.64% | 19.75% | | |
| *D. constrictiva* | 42.95% | 24.28% | 26.77% | 23.06% | 20.74% | 19.93% | 23.66% | 17.28% | 18.56% | 16.58% | 19.07% | 17.79% | |

**Table 4** Genetic distances for ITS-1 between the new species and its congeners

| | S. mediterranea | D. deharvengi | D. batuensis | D. bengalensis | D. notogaea | D. ryukyuensis | D. japonica | D. umbonata | D. circumcisa | D. verrucula | D. semiglobosa | D. majuscula | D. constrictiva |
|---|---|---|---|---|---|---|---|---|---|---|---|---|---|
| S. mediterranea | | | | | | | | | | | | | |
| D. deharvengi | 41.27% | | | | | | | | | | | | |
| D. batuensis | 39.50% | 9.59% | | | | | | | | | | | |
| D. bengalensis | 43.96% | 12.39% | 9.64% | | | | | | | | | | |
| D. notogaea | 44.85% | 13.39% | 10.41% | 1.07% | | | | | | | | | |
| D. ryukyuensis | 46.46% | 11.95% | 2.70% | 9.29% | 9.85% | | | | | | | | |
| D. japonica | 44.89% | 10.61% | 10.84% | 12.20% | 13.63% | 11.75% | | | | | | | |
| D. umbonata | 40.61% | 11.29% | 11.64% | 13.01% | 13.59% | 13.41% | 9.01% | | | | | | |
| D. circumcisa | 38.97% | 10.33% | 10.49% | 12.41% | 13.41% | 12.32% | 8.98% | 9.06% | | | | | |
| D. verrucula | 38.02% | 8.51% | 9.43% | 12.42% | 13.21% | 11.76% | 6.62% | 8.35% | 4.98% | | | | |
| D. semiglobosa | 39.08% | 9.96% | 12.20% | 14.33% | 15.56% | 14.48% | 9.55% | 11.05% | 5.48% | 6.00% | | | |
| D. majuscula | 37.96% | 8.67% | 9.58% | 11.14% | 12.33% | 12.36% | 5.84% | 7.78% | 4.80% | 2.77% | 5.30% | | |
| D. constrictiva | 38.39% | 10.74% | 10.20% | 12.88% | 13.64% | 12.65% | 6.82% | 8.19% | 6.38% | 2.61% | 7.77% | 3.44% | |
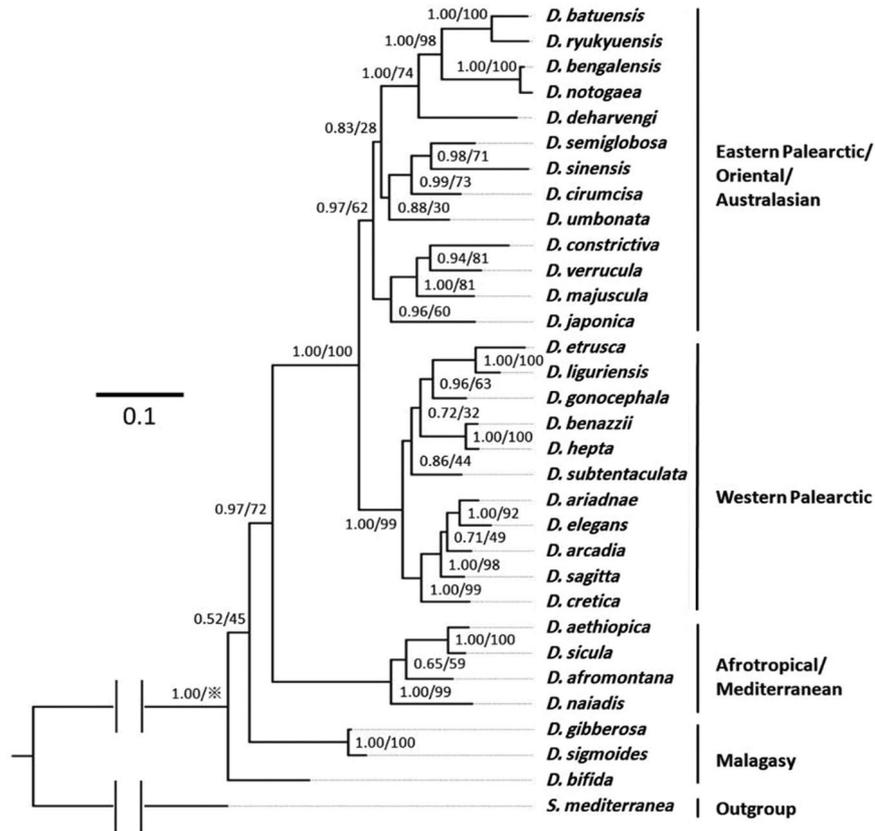
**Figure 2** Phylogenetic tree obtained from Bayesian analysis of the concatenated dataset. Numbers at nodes indicate support values (pp/bs). ※: Bootstrap value not applicable to the node because of different topologies of trees obtained by BI and ML methods. Scale bar: substitutions per site.

enlarged loops and mismatches of nucleotides occur in several tRNA genes of *D. constrictiva*. Furthermore, *tRNA S1* and *tRNA S2* show unorthodox structures (Fig. S3, Supporting Information).

For *D. constrictiva*, we identifiy 22 tRNA genes, which are arranged as follows: *cox1-E-nad6-nad5-S2-D-R-cox3-I-Q-K-atp6-V-nad1-W-cox2-P-nad3-A-nad2-M-H-F-rrnS-L1-Y-G-S1-rrnL-L2-T-atp8-C-N-cob-nad4l-nad4*. Mitochondrial gene order in other species of triclad (including incomplete and complete mitochondrial genomes) is shown in Fig. 4 (mitochondrial genes are ordered starting with *cox1*).

The concatenated alignment of the 12 protein-coding genes and 2 ribosomal genes is 10 475 base pairs (bp). The ML phylogenetic tree and its supporting values resulting from analysis of the concatenated dataset are similar to the BI tree and its values, differing only in nodes

weakly supported by at least one of the methodologies (Fig. 5; Fig. S4, Supporting Information). In this tree, Catenulida forms the basal branch, while the Neodermata forms the sister taxon of the Rhabditophora (including Macrostomorpha, Rhabdocoela, Polycladida, and Tricladida). The Tricladida is a well-supported monophyletic group, with the Maricola being sister to the other triclads (freshwater and land planarians) included in our dataset, in which the Dugesiidae are the sister taxon of the land planarians (Geoplanidae) (Fig. 5). In addition, the genus *Dugesia* is not recovered as monophyletic, neither in the BI nor in the ML inferred phylogeny. *Dugesia japonica* and *D. constrictiva* share a sister-group relationship, while *D. ryukyuensis* Kawakatsu, 1976, is sister to *Girardia* sp. instead of clustering with the other 2 *Dugesia* species (Fig. 5; Fig. S4, Supporting Information).
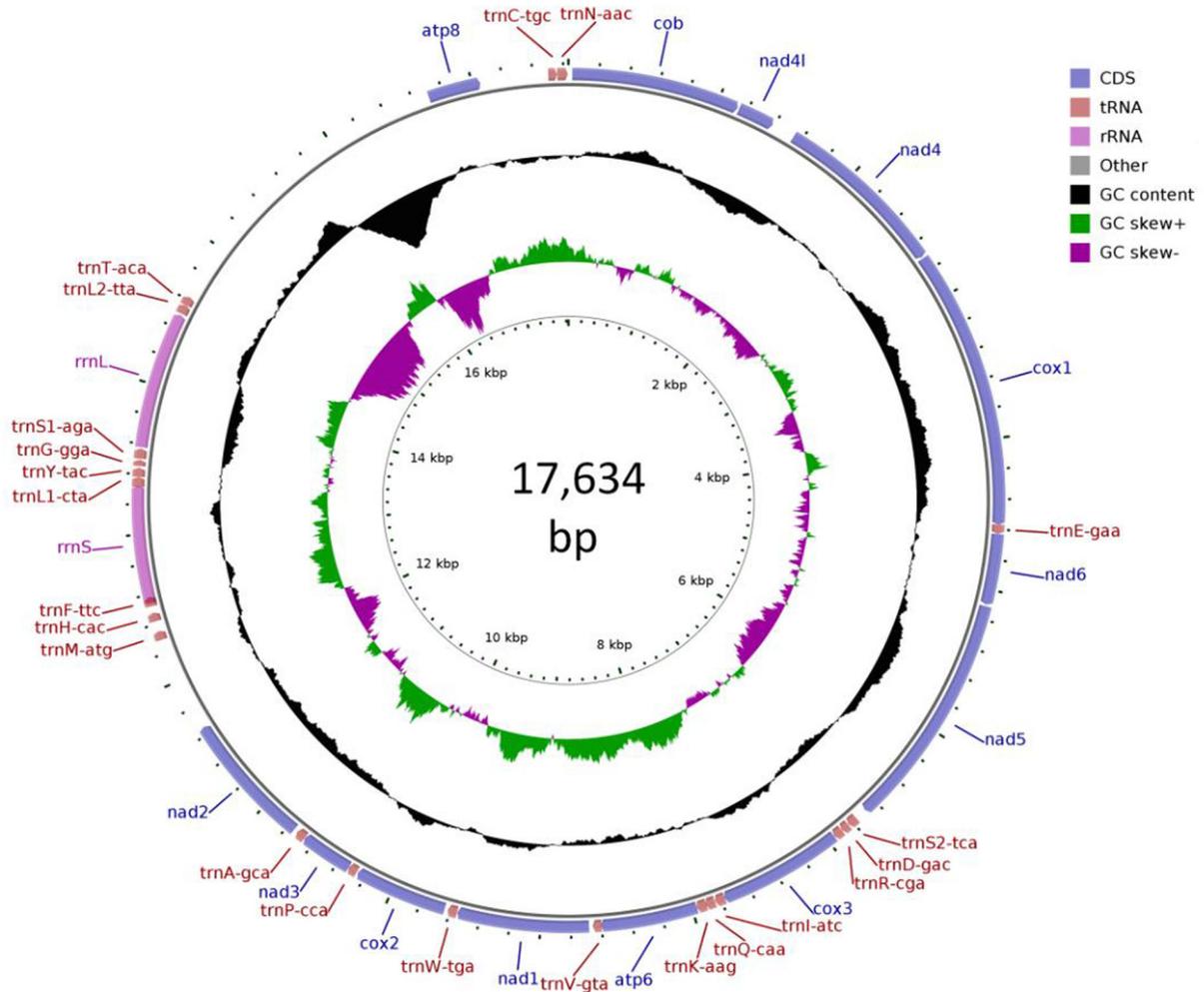
**Figure 3** Arrangement of the mitochondrial genome of *Dugesia constrictiva*. Abbreviations: atp6, ATP synthase F0 subunit 6; atp8, ATP synthase F0 subunit 8; cytb, Cytochrome *b*; cox1, Cytochrome c oxidase subunit I; cox2, Cytochrome *c* oxidase subunit II; cox3, Cytochrome *c* oxidase subunit III; nad1, NADH dehydrogenase subunit 1; nad2, NADH dehydrogenase subunit 2; nad3, NADH dehydrogenase subunit 3; nad4, NADH dehydrogenase subunit 4; nad4l, NADH dehydrogenase subunit 4L; nad5, NADH dehydrogenase subunit 5; nad6, NADH dehydrogenase subunit 6.

## Systematic account

Order Tricladida Lang, 1884

Suborder Continenticola Carranza, Littlewood, Clough, Ruiz-Trillo, Baguñà & Riutort, 1998

Family Dugesiidae Ball, 1974

Genus *Dugesia* Girard, 1850

*Dugesia constrictiva* Chen & Dong, **sp. nov.**

**Material examined**. Holotype: ZMHNU-HBYQ3, Yuquan village (35°43′5″N, 114°6′32′E), Taihang Mountains, Henan Provence, China, altitude: 205 m above sea level (a.s.l.), October 16, 2018, coll. G-W Chen, Z-M Dong and co-workers, sagittal sections on 27 slides.

Paratypes: ZMHNU-HBYQ1, ibid., sagittal sections on 20; RMNH VER. 19978.a, ibid., sagittal sections on 24 slides; RMNH VER. 19978.b, ibid., sagittal sections on 18 slides; ZMHNU-HBYQ5, ibid., sagittal sections on 18 slides; ZMHNU-HBYQ6, ibid., transverse sections on 23 slides; ZMHNU-HBYQ7, ibid., transverse sections on 24 slides; ZMHNU-HBYQ8, ibid., transverse sections on 34 slides; ZMHNU-HBYQ9, ibid., sagittal sections on 30 slides; ZMHNU-HBYQ10 and 11, ibid., horizontal sections on 20 and 17 slides, respectively.

**Figure 4** Gene order changes in mitochondrial genomes (from GenBank) in several species of triclad. Sequence for *D. constrictiva* generated in this study; for *D. japonica*, the corrected annotation in Solà *et al.* (2015) was used. Protein-coding genes in blue, tRNA genes in white, rRNA genes in grey. "?": noncanonical *atp8*.

**Diagnosis**. *Dugesia constrictiva* is characterized by the following features: asymmetrical openings of the oviducts; large, cuboidal copulatory bursa; vasa deferentia opening through ventro-lateral wall of the seminal vesicle; laterally compressed seminal vesicle; ventrally displaced ejaculatory duct, opening at the blunt tip of the penis papilla; long duct intercalated between seminal vesicle and diaphragm; chromosome complement diploid, with 16 metacentric chromosomes; mitochondrial gene order as follows: *cox1-E-nad6-nad5-S2-D-R-cox3-I-Q-K-atp6-V-nad1-W-cox2-P-nad3-A-nad2-M-H-F-rrnS-L1-Y-G-S1-rrnL-L2-T-atp8-C-N-cob-nad4l-nad4*.

**Etymology**. The specific epithet is derived from the Latin adjective *constrictivus*, drawn together, contracted, and alludes to the laterally compressed seminal vesicle.

**Habitat and reproduction**. The specimens were collected from a spring in the Taihang Mountains that had a water temperature of 20°C and was at an altitude of 205 m a.s.l. (Fig. 6a). Four animals were sexual at collection. After approximately 30 days of rearing under laboratory conditions, 10 sexually immature animals sexualized and laid spherical cocoons (about 0.7 mm in diameter), provided with a stalk. Newly laid cocoons were first dark red but later became brownish. After approximately 10 days, 3 to 5 young hatched from each cocoon. These juvenile worms were light brown and measured 2.1–2.9 mm in length and 0.3–0.4 mm in width.

**Description**. Living sexually immature animals measure 7–9 mm in length and 0.8–1.3 mm in width, while sexualized worms are 10–15 mm in length and 1–1.4 mm in width. The low triangular head is provided with 2 blunt auricles and with 2 eyes, which are located in pigment-free patches. Each eye cup houses numerous photoreceptor cells. The dorsal body surface is brown, excepting the pale body margins, while accumulations of pigment follow the outline of the pharyngeal pocket; ventral surface light brown (Fig. 6b).

Pharynx is located in the mid-region of the body, measuring about $1/6^{th}$ of the body length (Fig. 6b). Mouth opening locates at the posterior end of the pharyngeal pocket. Outer pharyngeal musculature is composed of a subepithelial layer of longitudinal muscles, followed by a layer of circular muscles; an extra inner layer of longitudinal muscles is not observed. The inner pharyngeal musculature consists of a subepithelial and thick layer of circular muscle, followed by a layer of longitudinal muscle.

Large and tall ventral ovaries are located at some distance behind the brain and often occupy over $1/2^{th}$ of the dorso-ventral space (Fig. 7a). For the sagitally sectioned specimens (ZMHNU HBYQ 1–5), we determine that the ovaries are located at about $1/6^{th}$—$1/7^{th}$ of the distance between the brain and the root of the pharynx. The infranucleated oviducts run ventrally in a caudayl direction to the level of the genital pore, after which they
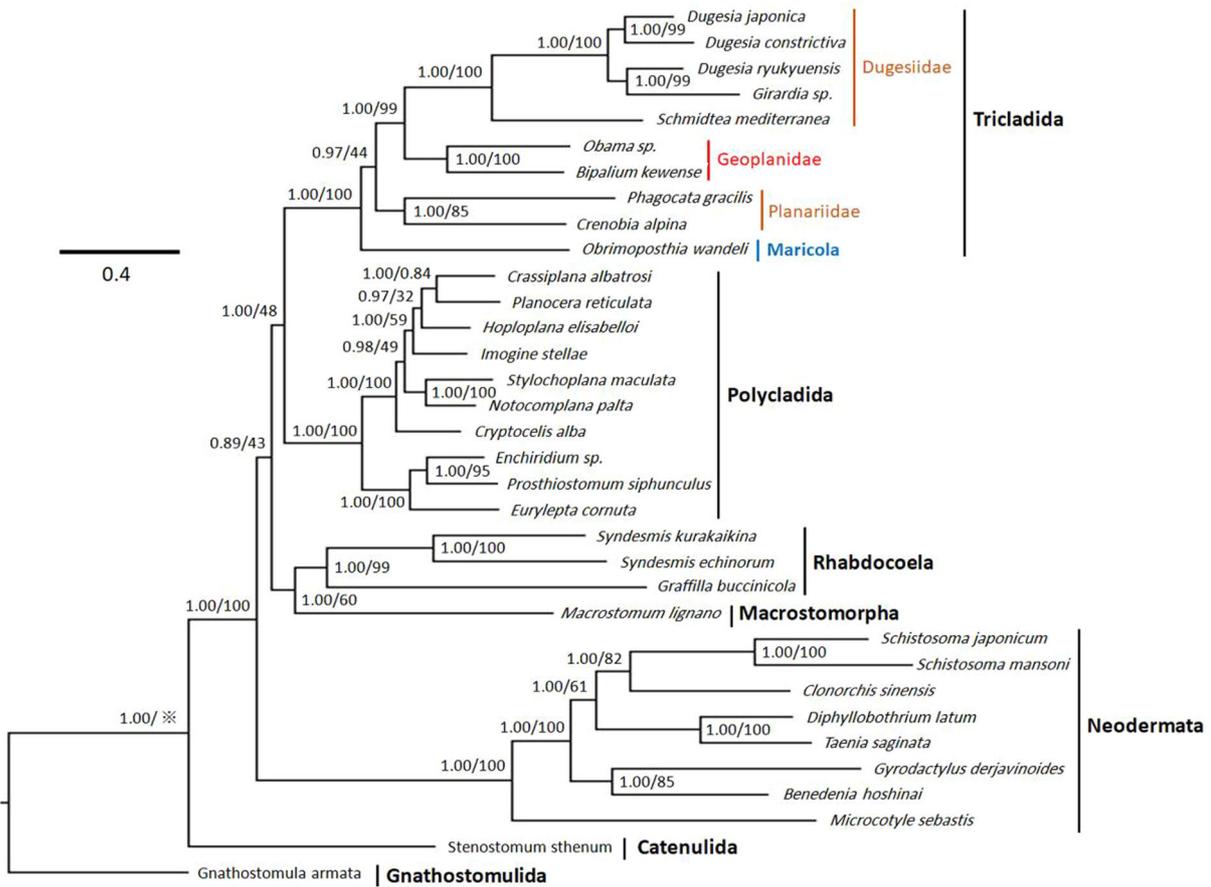
**Figure 5** Phylogenetic tree obtained from Bayesian analysis of the concatenated dataset for the protein-coding and rRNA genes within mitochondrial genomes. Numbers at nodes indicate support values (pp/bs). ※: Bootstrap value not applicable to the node because of different topologies of trees obtained by BI and ML methods. Scale bar: substitutions per site.
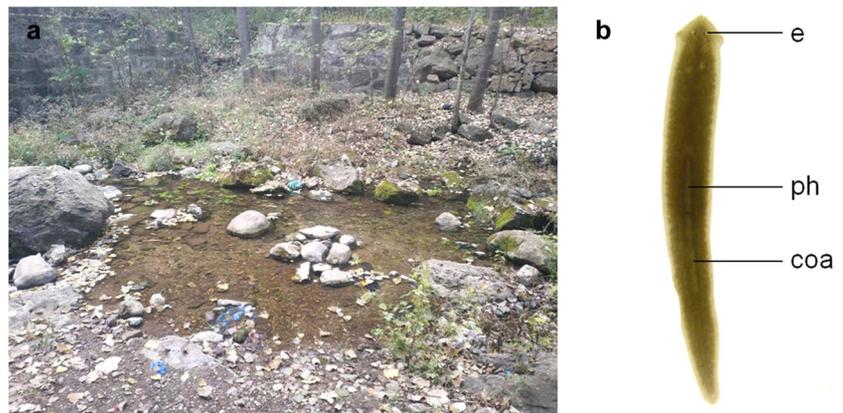


**Figure 6** Habitat and external appearance of *Dugesia constrictiva*. (a) Sampling site and habitat. (b) Sexually mature, live individual. Abbreviations: coa: copulatory apparatus; e: eye; ph: pharynx. Scale bar: 1 mm.

L. Wang *et al.*
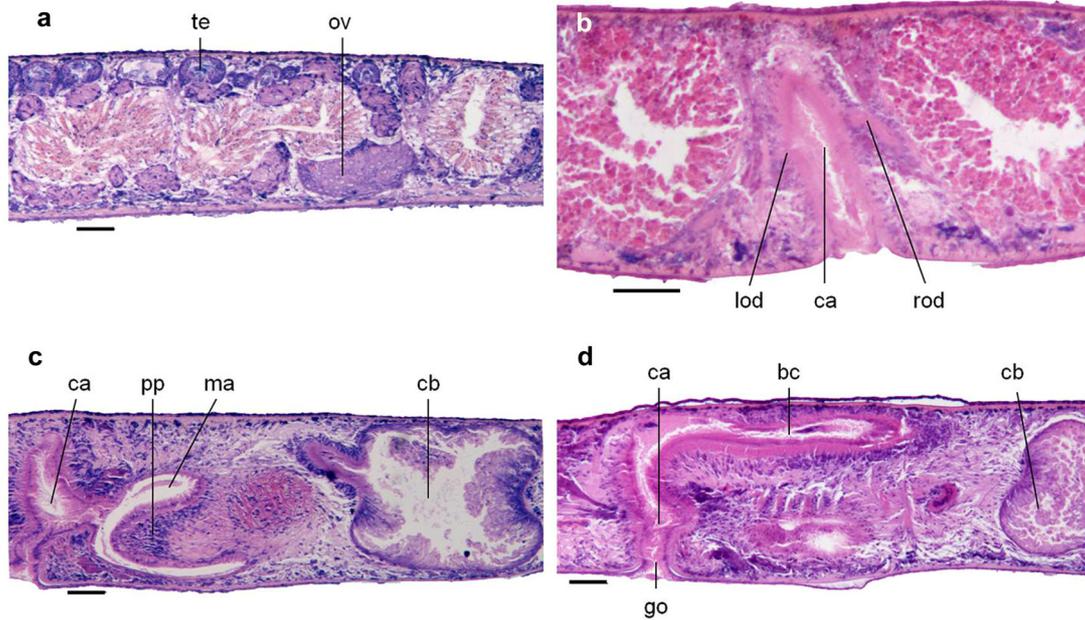


**Figure 7** *Dugesia constrictiva*. (a) Sagittal section of holotype ZMHNU-HBYQ 3, showing ovary and testes. (b) Transverse section of paratype ZMHNU-HBYQ 6, showing asymmetrical openings of the oviducts. (c) Sagittal section of holotype ZMHNU-HBYQ 3, showing the copulatory bursa. (d) Sagittal section of paratype ZMHNU-HBYQ 1, showing the bursal canal. Abbreviations: bc: bursal canal; ca: common atrium; cb: copulatory bursa; go: gonopore; lod: left oviduct; ma: male atrium; ov: ovary; pp: penis papilla; rod: right oviduct; te: testes. Scale bars: 100 μm.

curve dorso-medially to open separately and asymmetrically into the ventral portion of the bursal canal, with the left duct opens dorsally to the left one (Figs 7b, 9).

The large, more or less cuboidal copulatory bursa occupies the entire dorso-ventral space; it is lined by a columnar, vacuolated epithelium with basal nuclei and is devoid of any surrounding musculature (Figs 7c, 9). The bursal canal arises from the mid-posterior wall of the bursa and runs in a caudal direction to the left side of the male copulatory apparatus, after which it sharply bends ventrad and, subsequently, communicates with the common atrium (Figs 7c,d, 9). The bursal canal is lined with cylindrical, infranucleated, ciliated cells and is surrounded by a subepithelial layer of longitudinal muscles, followed by a layer of circular muscles that is particularly well developed on the ventral side of the canal. An extra outer layer of longitudinal musculature, forming the ectal reinforcement, extends from the vaginal region to about halfway along the bursal canal (Fig. 9). Erythrophil shell glands open into the vaginal region of the bursal canal around the oviducal openings.

The small testes are situated dorsally and are provided with mature spermatozoa (Fig. 7a). Testicular follicles extend from the posterior level of the ovaries to almost the posterior end of the body and are arranged in 4 to 5 longitudinal zones on either side of the midline of the body.

The vasa deferentia are filled with mature spermatozoa, and expand at the level of copulatory bursa to form spermiducal vesicles. When reaching the level of the penis bulb, the vasa deferentia sharply decrease in diameter and penetrate the antero-lateral wall of the penis bulb, whereafter the ducts traverse the bulb to open separately and symmetrically into ventro-lateral wall of the seminal vesicle (Figs 8b, 9). The sperm ducts are lined with nucleated cells and are surrounded by a layer of circular muscles. The relatively large seminal vesicle is lined by a flat, nucleated epithelium and is surrounded by a layer of intermingled muscle fibers. A characteristic feature of the seminal vesicle is that it is laterally compressed. This implies that in sagittal sections the first impression of the vesicle is that it corresponds to the usual normal, voluminous sac-shaped or globular structure present in other species. However, transverse and horizontal sections clearly reveal the seminal vesicle to be laterally compressed to such an extent that it actually attains the shape of a slot or long aperture (Fig. 8a,b). The posterior section of the seminal vesicle gives rise to a duct that via a comparatively large diaphragm opens into the ejaculatory
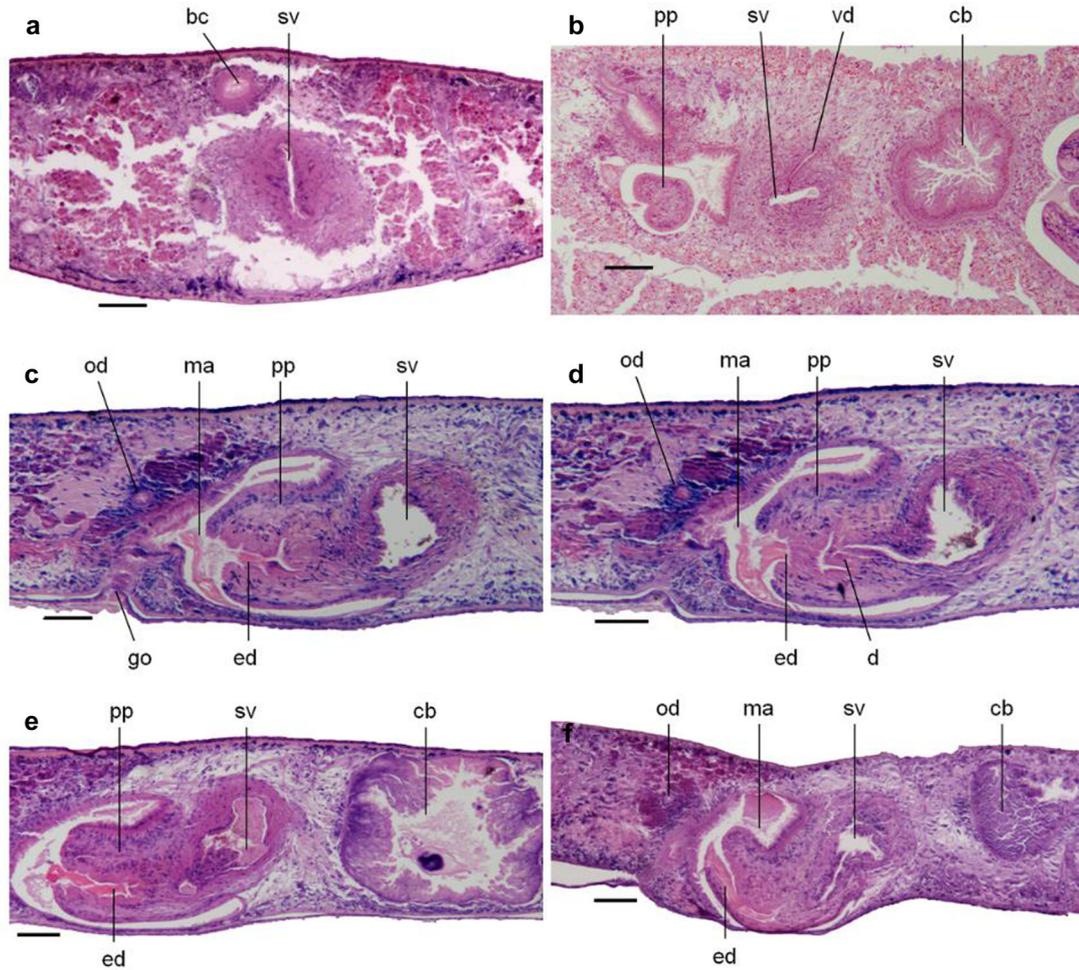
**Figure 8** *Dugesia constrictiva*. (a) Transverse section of paratype ZMHNU-HBYQ 6, showing the seminal vesicle. (b) Horizontal section of paratype ZMHNU-HBYQ 11, showing the seminal vesicle and opening of the vas deferens. (c) Sagittal section of holotype ZMHNU-HBYQ 3, showing the openings of ejaculatory duct, seminal vesicle and oviduct. (d) Sagittal section of holotype ZMHNU-HBYQ 3, showing the diaphragm and seminal vesicle. (e) Sagittal section of paratype ZMHNU-HBYQ 5, showing the copulatory bursa, ejaculatory duct and seminal vesicle. (f) Sagittal section of paratype ZMHNU-HBYQ 1, showing openings of the ejaculatory duct and seminal vesicle. Abbreviations: bc: bursal canal; cb: copulatory bursa; d: diaphragm; ed: ejaculatory duct; go: gonopore; ma: male atrium; od; oviduct; pp: penis papilla; sv: seminal vesicle; vd: vas deferens. Scale bars: 100 $\mu$m.

duct, which exits at the blunt tip of the penis papilla (Figs 8d,f, 9). The wall of the ejaculatory duct may show several folds. The diaphragm is located more or less halfway in the penis papilla. Both the intercalating duct between seminal vesicle and diaphragm and the ejaculatory duct are ventrally displaced, so that the penial papilla is asymmetrical, that is, with a large dorsal lip and a smaller ventral lip (Figs 8c–f, 9).

The stubby, cylindrical penis papilla is covered with an infranucleated epithelium that is underlain with a subepithelial layer of circular muscles, followed by a layer of longitudinal muscle fibers; the papilla is oriented more or less horizontally.

The genital atria comprises a common atrium and a male atrium, a female atrium virtually being absent. The common atrium communicates with a gonoduct that is lined by a columnar epithelium and receives the openings of abundant cement glands, and that leads the ventral gonopore (Figs 7d, 9).

## Karyology

Each of the 5 randomly selected specimens exhibits a diploid chromosome complement. In a total of 100 metaphase plates examined, 82 chromosome complements exhibit $2n = 2x = 16$ metacentric chromosomes
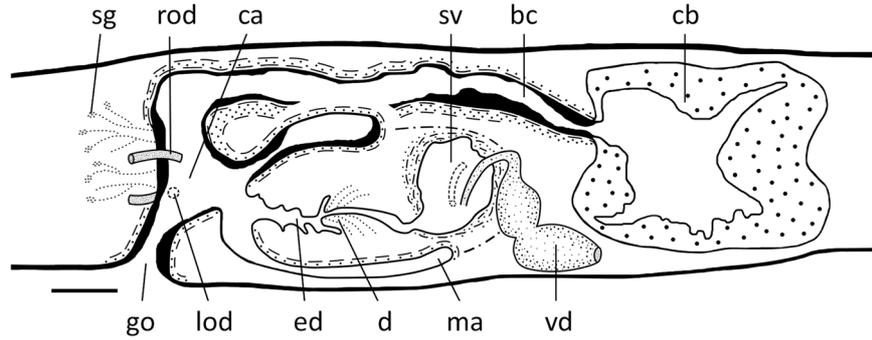
**Figure 9** *Dugesia constrictiva*. Sagittal reconstruction of the copulatory apparatus of the holotype. Abbreviations: bc: bursal canal; ca: common atrium; cb: copulatory bursa; d: diaphragm; ed: ejaculatory duct; go: gonopore; lod: left oviduct; ma: male atrium; rod: right oviduct; sg: shell glands; sv: seminal vesicle; vd: vas deferens. Scale bar: 100 $\mu$m.
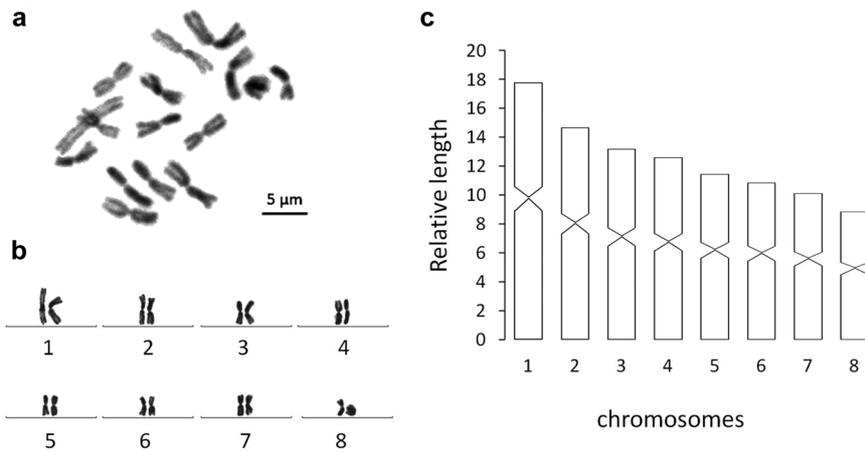


**Figure 10** *Dugesia constrictiva*. (a) Metaphasic plate. (b) Karyogram. (c) Idiogram. Scale bar: 5 $\mu$m.

(Fig. 10); chromosome complements of the remaining 18 plates cannot be determined, due to either lack of well-dispersed chromosomes or over-dispersed sets of chromosomes. Karyotype parameters, including the relative length, arm ratio, and centromeric index, are given in Table 5. The first pair of chromosomes is clearly larger than the others, being 1.88 times larger than the shortest chromosome. A chromosomal plate and idiogram of the karyotype are shown in Fig. 10.

## DISCUSSION

### Molecular phylogeny and genetic distances

The topology of our phylogenetic tree basically accords results from previous phylogenetic analyses (Lázaro *et al.* 2009; Solà *et al.* 2013; Stocchino *et al.* 2017; Song *et al.* 2020; Wang *et al.* 2021a,b). The Bayesian tree re-veals a sister-group relationship between a major clade comprising species from the Eastern Palearctic-Oriental-Australasian regions and one housing species from the Western Palearctic. In turn, these 2 clades together are sister to a clade comprising species from the Afrotropical-Mediterranean regions. The Malagasy clade forms a trichotomy at the base of the tree. As the tree is principally generated for determining the taxonomic status and phylogenetic position of *D. constrictiva* and because molecular information is available for only a limited number of species, it would be premature to use it for analyzing the historical biogeography of the genus *Dugesia* and, therefore, we do currently refrain from such an analysis.

Inter-specific genetic distances of COI and ITS-1 indicate that *D. constrictiva* is well-separated from other congeners. The lowest COI and ITS-1 distance values between *D. constrictiva* and other congeners are 17.79% and 3.44%, respectively (Table 3). The lowest COI distance

**Table 5** Karyotype parameters (mean values and standard deviations) of *Dugesia constrictiva*

| Chromosome | Relative length | Arm ratio | Centromeric index | Chromosome type |
|---|---|---|---|---|
| 1 | $17.81 \pm 0.44$ | $1.16 \pm 0.08$ | $46.38 \pm 1.75$ | m |
| 2 | $14.83 \pm 0.76$ | $1.11 \pm 0.08$ | $47.46 \pm 1.75$ | m |
| 3 | $13.41 \pm 0.33$ | $1.15 \pm 0.13$ | $46.62 \pm 2.64$ | m |
| 4 | $12.25 \pm 0.28$ | $1.29 \pm 0.11$ | $43.77 \pm 2.19$ | m |
| 5 | $11.49 \pm 0.66$ | $1.55 \pm 0.20$ | $39.41 \pm 3.11$ | m |
| 6 | $10.81 \pm 0.43$ | $1.28 \pm 0.14$ | $44.12 \pm 2.78$ | m |
| 7 | $10.09 \pm 0.28$ | $1.17 \pm 0.17$ | $46.28 \pm 3.22$ | m |
| 8 | $9.49 \pm 0.31$ | $1.21 \pm 0.11$ | $45.31 \pm 2.16$ | m |

m, metacentric.

values among species usually are between 6% and 10% (Làzaro *et al*. 2009; Solà *et al*. 2013; Stocchino *et al*. 2017; Harrath *et al*. 2019). For ITS-1, the lowest distance values that have been reported vary between 1% and 7% (Làzaro *et al*. 2009; Solà *et al*. 2013; Stocchino *et al*. 2017). Thus, the inter-specific genetic distances determined for *D. constrictiva* fall well outside of the range as determined previously for valid species of *Dugesia* and thus affirm its taxonomic status as a separate species and corroborate the anatomical and molecular phylogenetic results.

## Mitochondrial genome

### Gene order

It has been established that during the course of evolution, the *apt8* gene has been lost in neodermatan flatworms (McManus *et al*. 2004; Hardman & Hardman 2006). For a long time, it is actually assumed that *atp8* would be absent in all flatworms (Gissi *et al*. 2008; Podsiadlowski *et al*. 2014). However, recent studies show that planarians possess a noncanonical *atp8* (Ross *et al*. 2016; Egger *et al*. 2017; Monnens *et al*. 2020). In the present study, surprisingly, we find *atp8* indeed also in *D. constrictiva* and that it map between *rrnL* and *cob*, instead of mapping directly after *nad2*, as is the case in other Dugesiidae species (Fig. 4; see Ross *et al*. 2016; Egger *et al*. 2017). Although in the Planariidae species *Phagocata gracilis atp8* is also immediately followed by *nad2*, 2 other similar open reading frames (ORFs) of noncanonical *atp8* are located between *nad5* and *nad6* (Ross *et al*. 2016). Thus, position of the *atp8* gene is variable, at least in triclads. Furthermore, the amino acids of the protein sequence of the *atp8* gene, including the first 4 amino acids, are not conserved in planarians. Hoffmann *et al*. (1992) report that in the Metazoa the first 4 amino acids of the protein sequence of *atp8* are conserved, which are generally "MPQL". Nonetheless, the 4 amino acids are found to be divergent in recent studies. For instance, the protein sequence "MPHM" is found in several species of polyclads, "MVHT" in the planarian *S. mediterranea*, and "MVDV" in the planarian *P. gracilis* (Egger *et al*. 2017; Monnens *et al*. 2020). In summary, the *atp8* gene is highly divergent and generally short and, therefore, its identification and annotation are difficult.

With respect to the arrangement, the mitochondrial gene order of the new species and other triclad species (including incomplete and complete mitochondrial genomes) are shown in Fig. 4 (mitochondrial genes are ordered starting with *cox1*). Due to the lack of mitochondrial data from the Maricola, previous studies conclude that in triclads the order of protein-coding and ribosomal genes is conserved (Solà *et al*. 2015; Ross *et al*. 2016; Egger *et al*. 2017). In contrast, in the present study, we find that gene order exhibits significant differences between Maricola and Continenticola, with only the *cox2-nad3-nad2* block being conserved. The distinct differences of protein-coding and ribosomal gene order between Maricola and Continenticola concern 5 transpositions of the genes or gene-blocks (*rrnL*, *nad4l-nad4*, *nad6-nad5*, *cob*, and *nad1*; Fig. 4). Remarkably, however, protein-coding and ribosomal gene order is conserved in the mitochondrial genomes of freshwater planarians and land planarians of the suborder Continenticola, while occasionally a few tRNAs' rearrangements can be detected in the 3 families of the Continenticola (Geoplanidae, Dugesiidae, and Planariidae). For instance, there is no

rearrangement in the family Geoplanidae. In the superfamily Planarioidea, only one transposition of *tRNA C* is present between *Phagocata gracilis* (Haldeman, 1840) and *Crenobia alpina* (Dana, 1776). Several transpositions of tRNA are found in members of the family Dugesiidae. For example, transposition of *tRNA S1* is observed between *D. constrictiva* and *S. mediterranea*, and *tRNA C* transposition is found between *D. constrictiva* and *Girardia* sp. Our arrangement analyses show that tRNA transpositions can be found among the dugesiid genera *Dugesia*, *Girardia*, and *Schmidtea*, which accords with results from previous studies (see Sakai & Sakaizumi 2012; Solà *et al*. 2015; Ross *et al*. 2016). However, *D. constrictiva* also shows obvious tRNA transpositions as compared with its congeners, in that *tRNA E* and *tRNA N* are in different positions in *D. japonica*, while at least *tRNA N* is in a different position in *D. ryukyuensis* (Fig. 4). Our findings of *Dugesia* greatly differs from the conclusions of previous studies, which posited that mitochondrial gene rearrangement is absent in species of *Dugesia* (Sakai & Sakaizumi 2012; Solà *et al*. 2015; Ross *et al*. 2016).

Mitochondrial gene rearrangements may be extensive in certain Platyhelminthes, such as transpositions between the catenulids *Stenostomum sthenum* and *Stenostomum leucops* (Egger *et al*. 2017; Rosa *et al*. 2017). However, with respect to polyclad flatworms, *Imogine stellae* and *Imogine fafai* share a completely identical mitochondrial gene order (Kenny *et al*. 2018). With respect to rhabdocoels, *tRNA L1* and *tRNA L2* are different between *Syndesmis kurakaikina* and *Syndesmis echinorum* (Monnens *et al*. 2020). This illustrates the presence of mitochondrial gene rearrangements among species, thus suggesting a novel, supplementary marker for planarian taxonomy, albeit in other species gene order may be completely identical.

Presently, the taxonomy of planarians is mainly based on features of the reproductive system, which requires the availability of sexually mature specimens for taxonomic study. However, planarians frequently reproduce asexually by means of fission and, therefore, sexual specimens may be difficult to obtain under the natural conditions. In addition, induction of sexualization under laboratory conditions is difficult (Stocchino & Manconi 2013). Therefore, in such cases, analysis of the mitochondrial genome may contribute molecular markers for taxonomic and phylogenetic studies of triclad flatworms.

### Secondary structure

Up to now, putative secondary structures are determined for only 3 other planarians, namely, *D. japonica*, *C. alpina*, and *Obama* sp. (Sakai & Sakaizumi 2012; Solà *et al*. 2015). In *D. constrictiva*, most of the tRNAs are equipped with 4 arms, but *tRNA S1* and *tRNA S2* lack the D arm, a condition is also found in the above-mentioned 3 species. However, excessively enlarged loops of *tRNA S1* and *tRNA S2* are not found in these 3 species, but are present in *D. constrictiva*. Such rare secondary structures have been reported in the literature for only a few other flatworms, such as *Graffilla buccinicola* Jameson, 1897 (*tRNA V*, see Monnens *et al*. 2020) and *Macrostomum lignano* Ladurner *et al*. 2005 (*tRNA Q*, see Egger *et al*. 2017). In view of the paucity of data on secondary structures of tRNA in planarian species, we defer more comprehensive discussion to a later date, when a wider taxonomic coverage is available.

### Phylogenetic tree of protein coding and rRNA genes

The major function of the phylogenetic tree created on the basis of the concatenated alignment of the 12 protein-coding genes and 2 ribosomal genes (Fig. 5) is to determine the phylogenetic relationships within the Tricladida, as well those between the triclads and other taxa of the Platyhelminthes. Evidently, lack of information does not allow inclusion of more planarian species, so that even some higher taxa are not represented in our tree, for example, Cavernicola. Nevertheless, the gross topology of the triclad phylogeny in Fig. 5 is basically consistent with several studies that over the years have developed theories on the taxonomy and evolution of the triclad flatworms (see Sluys & Riutort 2018 and references therein). The most recent analyses, which include also members of the suborder Cavernicola, reveale that the latter are sister to the Maricola and that together they share a sister-group relationship with the Continenticola, the latter comprising all land planarians (family Geoplanidae) and members of the freshwater planarian family Dugesiidae (Benítez-Álvarez *et al*. 2020; Stocchino *et al*. 2021), similar to our tree (Fig. 5). According to Benítez-Álvarez *et al*. (2020), continenticolans evolve from a freshwater ancestor. Unfortunately, there are very few calibrated timetrees available for triclad flatworms, but those that have been generated suggest that continenticolans form an ancient clade; by implication, the same must then hold true for the other suborders of the Tricladida (Làzaro *et al*. 2011; Solà *et al*. 2013). Significantly, our results fail to recover the genus *Dugesia* as a monophyletic clade, due to the fact that *D. ryukyuensis* constitutes the sister-species of *Girardia* sp. This relationship is also reported in previous mitochondrial phylogenetic studies, in which

*Girardia* sp. always shares a sister-group relationship with *D. ryukyuensis*, the latter thus failing to group with its congeners (Gastineau *et al*. 2019; Yang *et al*. 2019; Monnens *et al*. 2020). However, in others, phylogenetic studies, based on either morphological or molecular markers, show that *Girardia* constitutes a basal branch than the genera *Dugesia* and *Schmidtea* of the family Dugesiidae (De Vries & Sluys 1991; Sluys *et al*. 1998; Álvarez-Presas *et al*. 2008; Sluys & Riutort 2018). These discrepancies may simply be due to the fact that the various phylogenetic studies use different datasets and different methodologies, which may easily lead to contradictory results (Cameron *et al*. 2009; Cheng *et al*. 2010).

## Morphology

A central or ventrally displaced course of the ejaculatory duct and a terminal or subterminal opening of the duct at the tip of the penis papilla form important taxonomic characters in the identification of species of *Dugesia* and for resolution of phylogenetic relationships within the genus (cf. Sluys *et al*. 1998). In particular, the feature concerning the course of the ejaculatory duct is not always correctly described and/or interpreted in taxonomic accounts on species of *Dugesia* and, therefore, Stocchino *et al*. (2017) have precisely defined this character state and then re-assessed it in 16 species. Another important character concerns the absence or presence of a duct intercalated between the seminal vesicle and the diaphragm (character state 5-1 in Sluys *et al*. 1998).

In *D. constrictiva*, there are a ventrally displaced ejaculatory duct, with a terminal opening, as well as a duct between seminal vesicle and diaphragm, a combination of character states that is present also in the following species: *D. borneana* Kawakatsu, 1972, *D. ectophysa* Marcus, 1953, *D. hymanae* (Sivickis, 1928), *D. mertoni* (Steinmann, 1914), *D. notogaea* Sluys & Kawakatsu, 1998, *D. ryukyuensis, D. siamana* Kawakatsu, 1980 (see Sluys *et al*. 1998; Stocchino *et al*. 2017). Among these species, only *D. constrictiva*, *D. ectophysa*, and *D. notogaea* have oviducts that open asymmetrically into the bursal canal. However, the penis bulb of *D. ectophysa* is completely different from that present in *D. constrictiva* in that it consists of an elongated, highly muscular structure that is located near the ventral body wall (Marcus 1953). In *D. notogaea*, the sperm ducts open through the mid-anterior wall of the seminal vesicle, whereas in *D. constrictiva* the ducts open into the postero-ventral part of the vesicle. Therefore, *D. constrictiva* cannot be equated with either *D. notogaea* or *D. ectophysa*.

## Karyology

The new species *D. constrictiva* shows a haploid number of $n = 8$, in correspondence with the conclusion of Stocchino *et al*. (2004) that in the genus *Dugesia* the basic chromosome number is 7, 8, or 9, while all of its chromosomes are metacentric.

Chromosome portraits is similar to the one of *D. constrictiva* have been documented also for the following species: many Sardinian populations of *D. benazzii* Lepori, 1951, *D. etrusca labronica* Lepori, 1950, *D. elegans* de Vries, 1984, *D. gonocephala* (Dugès, 1830), *D. japonica*, *D. indonesiana*, *D. majuscula*, *D. sagitta* (Schmidt, 1861), *D. semiglobosa*, *D. circumcisa*, *D. verrucula*, *D. salina* (Whitehouse, 1913), and presumably also *D. colapha* Dahm, 1967 (cf. Dahm 1967; Benazzi & Gourbault 1975; Kawakatsu *et al*. 1976; Ball 1979; De Vries 1984; Deri *et al*. 1999; Pala *et al*. 1999; Stocchino 2018; Wang *et al*. 2021a,b; Bromley-Schnur 2021). Evidently, none of these species is anatomically similar to *D. constrictiva*; otherwise, we would have included these in our comparative morphological discussion (see above). In view of the fact that *D. constrictiva* exhibits a diploid chromosome portrait and, thus, most likely, shows regular meiosis, it is unsurprising that it reproduces sexually and produces cocoons.

## ACKNOWLEDGMENTS

## CONFLICT OF INTEREST

The authors declare no conflict of interest.

## REFERENCES

Abascal F, Zardoya R, Telford MJ (2010). TranslatorX: Multiple alignment of nucleotide sequences guided by amino acid translations. *Nucleic Acids Research* **38**, W7–13.

Álvarez-Presas M, Baguñà J, Riutort M (2008). Molecular phylogeny of land and freshwater planarians (Tricladida, Platyhelminthes): From freshwater to land

and back. *Molecular Phylogenetics & Evolution* **47**, 555–68.

Ball IR (1979). The karyotypes of two *Dugesia* species from Corfu, Greece (Platyhelminthes, Turbellaria). *Bijdragen tot de Dierkunde* **48**, 187–90.

Benazzi M, Gourbault N (1975). Cytotaxonomical study of *Dugesia indonesiana* Kawakatsu (Tricladida Paludicola). *Atti della Accademia Nazionale dei Lincei. Classe di Scienze Fisiche, Matematiche e Naturali. Rendiconti* **58**, 237–43.

Benítez-Álvarez L, Maria Leal-Zanchet A, Oceguera-Figueroa A (2020). Phylogeny and biogeography of the Cavernicola (Platyhelminthes: Tricladida): Relics of an epigean group sheltering in caves? *Molecular Phylogenetics and Evolution* **145**, 106709.

Bromley-Schnur HJ (2021). The genus *Phagocata* Leidy (Platyhelminthes, Tricladida) in Israel, a new species of *Phagocata* from Lake Kinneret, and an emended description of *Dugesia salina*. *Zootaxa* **4969**, 293–317.

Cameron SL, Sullivan J, Song H, Miller KB, Whiting MF (2009). A mitochondrial genome phylogeny of the Neuropterida (lace-wings, alderflies and snakeflies) and their relationship to the other holometabolous insect orders. *Zoologica Scripta* **38**, 575–90.

Castresana J (2000). Selection of conserved blocks from multiple alignments for their use in phylogenetic analysis. *Molecular Biology and Evolution* **17**, 540–52.

Chen G-W, Wang Y-L, Wang H-K, Fu R-M, Zhang J-F, Liu D-Z (2008). Chromosome and karyotype analysis of *Polycelis wutaishanica* (Turbellaria, Tricladida) from Shanxi province, China. *Acta Zootaxonomica Sinica* **33**, 449–52.

Chen Y-H, Chen X-M, Wu C-C, Wang A-T (2015). A new species of the genus *Dugesia* (Tricladida, Dugesiidae) from China. *Zoological Systematics* **40**, 237–49.

Cheng Y, Xu T, Ge S, Wang R (2010). Complete mitochondrial genome of the miiuy croaker *Miichthys miiuy* (Perciformes, Sciaenidae) with phylogenetic consideration. *Marine Genomics* **3**, 201–9.

Dahm AG (1967). A new *Dugesia* "microspecies" from Ghana belonging to the *Dugesia gonocephala* group – Turbellaria Tricladida Paludicola. *Arkiv för Zoologi* **19**, 309–21.

Deri P, Colognato R, Rossi L, Salvetti A, Batistoni R (1999). A karyological study on populations of *Dugesia gonocephala* s.l. (Turbellaria, Tricladida). *Italian Journal of Zoology* **66**, 245–53.

Dessimoz C, Gil M (2010). Phylogenetic assessment of alignments reveals neglected tree signal in gaps. *Genome Biology* **11**, R37.

De Vries EJ (1984). On the karyology of *Dugesia gonocephala* s.l. (Turbellaria, Tricladida) from Montpellier, France. *Hydrobiologia* **132**, 251–6.

De Vries EJ, Sluys R (1991). Phylogenetic relationships of the genus *Dugesia* (Platyhelminthes, Tricladida, Paludicola). *Journal of Zoology, London* **223**, 103–16.

Dong Z-M, Chen G-W, Zhang H-C, Liu D-Z (2017). A new species of *Polycelis* (Platyhelminthes, Tricladida, Planariidae) from China. *Acta Zoologica Academiae Scientiarum Hungaricae* **63**, 263–76.

Egger B, Bachmann L, Fromm B (2017). Atp8 is in the ground pattern of flatworm mitochondrial genomes. *BMC Genomics* **18**, 414.

Gastineau R, Justine J, Lemieux C, Turmel M, Witkowski A (2019). Complete mitogenome of the giant invasive hammerhead flatworm *Bipalium kewense*. *Mitochondrial DNA Part B* **4**, 1343–4.

Gissi C, Iannelli F, Pesole G (2008). Evolution of the mitochondrial genome of Metazoa as exemplified by comparison of congeneric species. *Heredity* **101**, 301–20.

Hardman M, Hardman LM (2006). Comparison of the phylogenetic performance of neodermatan mitochondrial protein-coding genes. *Zoologica Scripta* **35**, 655–65.

Harrath AH, Sluys R, Mansour L *et al.* (2019). Molecular and morphological identification of two new African species of *Dugesia* (Platyhelminthes, Tricladida, Dugesiidae) from Cameroon. *Journal of Natural History* **53**, 253–71.

Hoffmann RJ, Boore JL, Brown WM (1992). A novel mitochondrial genome organization for the blue mussel, *Mytilus edulis*. *Genetics* **131**, 397–412.

Katoh K, Standley DM (2013). MAFFT multiple sequence alignment software version 7: Improvements in performance and usability. *Molecular Biology and Evolution* **30**, 772–80.

Kawakatsu M, Oki I, Tamura S, Sugino H (1976). Studies on the morphology, karyology and taxonomy of the Japanese freshwater planarian *Dugesia japonica* Ichikawa et Kawakatsu, with a description of a new subspecies. *Dugesia japonica ryukyuensis* subspec. nov. *The Bulletin of Fuji Women's College* **14**, 81–126.

Kenny NJ, Noreña C, Damborenea C, Grande C (2018). Probing recalcitrant problems in polyclad evolution and systematics with novel mitochondrial genome resources. *Genomics* **111**, 343–55.

Kück P, Meusemann K (2010). FASconCAT: Convenient handling of data matrices. *Molecular Phylogenetics and Evolution* **56**, 1115–8.

Lázaro EM, Harrath AH, Stocchino GA, Pala M, Riutort M (2011). *Schmidtea mediterranea* phylogeography: An old species surviving on a few Mediterranean islands? *BMC Evolutionary Biology* **11**, 274.

Lázaro EM, Sluys R, Pala M, Stocchino GA, Baguñà J, Riutort M (2009). Molecular barcoding and phylogeography of sexual and asexual freshwater planarians of the genus *Dugesia* in the Western Mediterranean (Platyhelminthes, Tricladida, Dugesiidae). *Molecular Phylogenetics and Evolution* **52**, 835–45.

Levan A, Fredga K, Sandberg AA (1964). Nomenclature for centromeric position on chromosomes. *Hereditas* **52**, 201–20.

Lin W, Wang F, Yang J-H *et al*. (2020). Meso-Cenozoic u evidence from zircon and apatite thermochronology evidence from zircon and apatite thermochronology and apatite thermochronology. *Geological Magazine* **157**, 1097–1111.

Littlewood DTJ, Telford MJ, Clough KA, Rohde K (1998). Gnathostomulida-an enigmatic metazoan phylum from both morphological and molecular perspectives. *Molecular Phylogenetics and Evolution* **9**, 72–9.

Marcus E (1953). Turbellaria Tricladida. In: Exploration du Parc National de l'Upemba, Mission G. F. de Witte, Fasc. 21, Bruxelles: 1–62.

McManus DP, Le TH, Blair D (2004). Genomics of parasitic flatworms. *International Journal for Parasitology* **34**, 153–8.

Monnens M, Thijs S, Briscoe AG *et al*. (2020). The first mitochondrial genomes of endosymbiotic rhabdocoels illustrate evolutionary relaxation of atp8 and genome plasticity in flatworms. *International Journal of Biological Macromolecules* **162**, 454–69.

Pala M, Casu S, Stocchino G (1999). Karyology and karyotype analysis of diploid freshwater planarian populations of the *Dugesia gonocephala* group (Platyhelminthes, Tricladida) found in Sardinia. *Hydrobiologia* **392**, 113–9.

Podsiadlowski L, Mwinyi A, Lesný P, Bartolomaeus T (2014). Mitochondrial gene order in Metazoa - theme and variations. In: Wägele JW, Bartolomaeus T, eds. *Deep Metazoan Phylogeny: The Backbone of the Tree of Life. New insights from Analyses of Molecules, Morphology, and Theory of Data Analysis*. De Gruyter, Inc, Berlin, pp. 459–72.

Raorao MO, Yan Y, Wang G, Li W-H, Murnyi D (2019). Holomorphology of *Kamimuria peppapiggi*a sp. n. (Plecoptera: Perlidae) from the foothills of Taihang Mountains, Henan Province of China. *Zootaxa* **4668**, 575–87.

Ronquist F, Teslenko M, van der Mark P *et al*. (2012). MrBayes 3.2: efficient Bayesian phylogenetic inference and model choice across a large model space. *Systematic Biology* **61**, 539–42.

Rosa MT, Oliveira DS, Loreto ELS (2017). Characterization of the first mitochondrial genome of a catenulid flatworm: *Stenostomum leucops* (Platyhelminthes). *Journal of Zoological Systematics and Evolutionary Research* **55**, 98–105.

Ross E, Blair D, Guerrero-Hernandez C, Alvarado AS (2016). Comparative and transcriptome analyses uncover key aspects of coding- and long noncoding RNAs in flatworm mitochondrial genomes. *Genes Genomes Genetics* **6**, 1191–200.

Sakai M, Sakaizumi M (2012). The complete mitochondrial genome of *Dugesia japonica* (Platyhelminthes; Order Tricladida). *Zoological Science* **29**, 672–80.

Sluys R, Kawakatsu M, Winsor L (1998). The genus *Dugesia* in Australia, with its phylogenetic analysis and historical biogeography (Platyhelminthes, Tricladida, Dugesiidae). *Zoologica Scripta* **27**, 273–90.

Sluys R, Riutort M (2018). Planarian diversity and phylogeny. In: Rink JC, ed. *Planarian Regeneration: Methods and Protocols. Methods in Molecular Biology*, Vol. 1774. Humana Press, Springer Science+Business Media, New York, pp. 1–56. https://doi.org/10.1007/978-1-4939-7802-1_1

Solà E, Álvarez-Presas M, Frías-López C *et al*. (2015). Evolutionary analysis of mitogenomes from parasitic and free-living flatworms. *PLoS ONE* **10**, e0120081.

Solà E, Sluys R, Gritzalis K, Riutort M (2013). Fluvial basin history in the northeastern Mediterranean region underlies dispersal and speciation patterns in the genus *Dugesia* (Platyhelminthes, Tricladida, Dugesiidae). *Molecular Phylogenetics and Evolution* **66**, 877–88.

Song X-Y, Li W-X, Sluys R, Huang S-X, Wang A-T (2020). A new species of *Dugesia* (Platyhelminthes, Tricladida, Dugesiidae) from China, with an account on the histochemical structure of its major nervous system. *Zoosystematics and Evolution* **96**, 431–47.

Stamatakis A (2014). RAxML version 8: A tool for phylogenetic analysis and post-analysis of large phylogenies. *Bioinformatics (Oxford, England)* **30**, 1312–3.

Stocchino GA (2018). 80 years of research on planarians (Platyhelminthes, Tricladida) from Sardinia, Italy: An annotated checklist. *Zootaxa* **4532**, 539–52.

Stocchino GA, Dols-Serrate D, Sluys R, Riutort M, Onnis C, Manconi R (2021). Amphibioplanidae: a new branch and family on the phylogenetic tree of the triclad flatworms (Platyhelminthes: Tricladida), represented by a species from Sardinian caves with a remarkable lifestyle. *Zoological Journal of the Linnean Society* **183**, https://doi.org/10.1093/zoolinnean/zlaa183

Stocchino GA, Manconi R (2013). Overview of life cycles in model species of the genus *Dugesia* (Platyhelminthes Tricladida). *Italian Journal of Zoology* **80**, 319–28.

Stocchino GA, Manconi R, Corso G, Pala M (2004). Karyology and karyometric analysis of an Afrotropical freshwater planarian (Platyhelminthes, Tricladida). *Italian Journal of Zoology* **71**, 89–93.

Stocchino GA, Sluys R, Riutort M, Solà E, Manconi R (2017). Freshwater planarian diversity (Platyhelminthes: Tricladida: Dugesiidae) in Madagascar: New species, cryptic species, with a redefinition of character states. *Zoological Journal of the Linnean Society* **181**, 727–56.

Talavera G, Castresana J (2007). Improvement of phylogenies after removing divergent and ambiguously aligned blocks from protein sequence alignments. *Systematic Biology* **56**, 564–77.

Tamura K, Stecher G, Peterson D, Filipski A, Kumar S (2013). MEGA6: Molecular evolutionary genetics analysis version 6.0. *Molecular Biology and Evolution* **30**, 2725–9.

Tan G, Muffato M, Ledergerber C *et al*. (2015). Current methods for automated filtering of multiple sequence alignments frequently worsen single-gene phylogenetic inference. *Systematic Biology* **64**, 778–91.

Wang B, Jiang J, Xie F *et al*. (2009). Molecular phylogeny and genetic identification of populations of two species of *Feirana* frogs (Amphibia: Anura, Ranidae, Dicroglossinae, Paini) endemic to China. *Zoological Science* **26**, 500–9.

Wang L, Chen J-Z, Dong Z-M, Chen G-W, Sluys R, Liu D-Z (2021a). Two new species of *Dugesia* (Platyhelminthes, Tricladida, Dugesiidae) from the tropical monsoon forest in southern China. *ZooKeys* **1059**, 89–116.

Wang L, Dong Z-M, Chen G-W, Sluys R, Liu D-Z (2021b). Integrative descriptions of two new species of *Dugesia* from Hainan Island, China (Platyhelminthes, Tricladida, Dugesiidae). *ZooKeys* **1028**, 1–28.

Yang H-M, Ji S-J, Min G-S (2019). The complete mitochondrial genome of the Antarctic marine triclad, *Obrimoposthia Wandeli* (Platyhelminthes, Tricladida, Maricola). *Mitochondrial DNA Part B* **4**, 2515–6.

Zhong H-W, Zhao X, Yin S-M, Zhao X, Zhao T (2010). Late Cenozoic geomorphology, geochronology and physiography of Yuntaishan in Southern Taihang Mountain, North China. *Bulletin of the Geological Society of China* **84**, 230–9.

## SUPPLEMENTARY MATERIALS

Additional supporting information may be found online in the Supporting Information section at the end of the article.

**Table S1** Primers used for amplification, and their annealing temperatures

**Table S2** Mitochondrial genomes used for homologous alignments

**Figure S1** Phylogenetic tree obtained from ML analysis of the concatenated dataset. Numbers at nodes indicate support values (bootstrap). Scale bar: substitutions per site.

**Figure S2** The transmembrane domain of *atp8* gene (in blue) predicted by SMART.

**Figure S3** Putative secondary structures of mitochondrial tRNA for *Dugesia constrictiva*.

**Figure S4** Phylogenetic tree obtained from ML analysis of the concatenated dataset for the protein-coding and rRNA genes within mitochondrial genomes. Numbers at nodes indicate support values (bootstrap). Scale bar: substitutions per site.

**Cite this article as:**

Wang L, Wang Y, Dong Z, Chen G, Sluys S, Liu D (2021). Integrative taxonomy unveils a new species of *Dugesia* (Platyhelminthes, Tricladida, Dugesiidae) from the southern portion of the Taihang Mountains in northern China, with the description of its complete mitogenome and an exploratory analysis of mitochondrial gene order as a taxonomic character. *Integrative Zoology* **00**, 1–22.